SOVIET PHYSICS USPEKHI VOLUME 12, NUMBER 6 MAY-JUNE 1970

537.523/.527

New Instruments and Measurements Methods

HIGH-FREQUENCY HIGH-PRESSURE INDUCTION DISCHARGE AND THE ELECTRODELESS PLASMOTRON

Yu. P. RAĬZER

Institute of Mechanics Problems, USSR Academy of Sciences

Fiz. Nauk 99, 687–712 (December, 1969)

I. INTRODUCTION

THE phenomenon of high-frequency induction (electrodeless) discharge in gases has been known since the end of the last century. However, it was not immediately understood. The induction discharge is easy to observe if an evacuated vessel is placed inside a solenoid carrying a sufficiently strong high-frequency current. Under the influence of the vortical electric field induced by the alternating magnetic flux, breakdown is produced in the residual gas and a discharge is ignited. The discharge (ionization) is maintained at the expense of the Joule heat of the annular induction current flowing in the ionized gas along the force lines of the vortical electric field (the magnetic force lines inside a long solenoid are parallel to the axis; Fig. 1).

Among the older papers on electrodeless discharge (reference to which can be found in[1,2]), the most thorough investigations were reported by J. J. Thomson[2] who, in particular, demonstrated experimentally the induction nature of the discharge and derived the theoretical conditions for its ignition, namely, the dependence of the breakdown-threshold magnetic field on the gas pressure (and on the frequency). The ignition curves have a minimum, in analogy with the Paschen curves for the breakdown of a discharge gap in a constant electric field. For the practical frequency range (from several tenths to several dozen MHz), the minimum lie in the low-pressure region; the discharge is usually observed only in strongly rarefied gases.

A high frequency discharge of another, capacitive type, has been known for a long time. Such a discharge is produced in an evacuated vessel placed between the plates of a capacitor connected to an oscillating circuit. A characteristic feature of capacitive-type discharges is the fact that the force lines of the high-frequency electric field are not closed in the discharge zone.

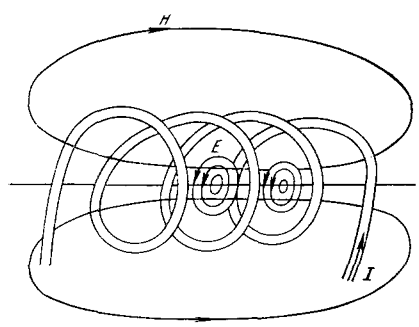

FIG. 1. Diagram of fields in the solenoid.

In the present article we shall consider only inductive discharges, and furthermore high-pressure discharges, which have found important practical applications as means of obtaining a dense pure plasma; this plasma is subsequently used for a variety of purposes. The principal scheme of the process does not differ, in essence, from the experiment described in the very beginning of this article. The inductive discharge is produced inside a solenoid (inductor), but to maintain the discharge at high atmospheric pressure of the gas, large powers are needed, on the order of several kilowatts. In this case the plasma temperature is on the order of 10,000°K.

A stationary static discharge regime is possible, wherein the heat fed to the immobile plasma electromagnetically is dissipated by heat conduction through the cooled walls of the vessel. However, greatest interest attaches to the regime in which the cold gas is blown through the solenoid, is heated in a stationary hot discharge, and leaves the inductor in the form of a dense plasma jet at atmospheric pressure, with the process continuing for a prolonged time. Such a device is called an inductive plasma burner or an electrodeless plasmotron*.

Electrodeless plasmatrons have certain important advantages over the more widely used arc plasmatrons, in which the electric energy is introduced in the gas stream by means of an arc discharge. First, in the electrodeless plasmotron there is produced a pure sterile plasma, not contaminated by the electrode-erosion product; the obtained plasma jet is more stable and the operating time is practically unlimited, whereas in arc plasmatrons of high power the electrodes are rapidly disintegrated.

Electrodeless plasmotrons find increasing application in physics research and in engineering, such as plasma chemistry, metallurgy, the growing of crystals of refractory substances, in other words, wherever a pure and uncontaminated dense plasma is needed. All this has attracted the attention of many physicists and engineers in all leading countries to the electrodeless high-pressure discharge.

It must be stated that in this field the technical process has noticeably influenced the understanding of the

*It should be noted that the principle of heating conducting bodies by induced high-frequency currents (eddy currents) has been in use in technology for a long time. It is the basis of a great variety of melting furnaces, apparatus for heat treatment of metal articles, etc. From the purely dynamic point of view, the process occurring here is in essence the same as in the inducted discharge in a gas.

physical nature and the theory of the occurring phenomena. Powerful installations are already in operation, but much of the information needed for the effective selection of their parameters and operating conditions has been obtained empirically, whereas a serious study of the theory of the processes was initiated only in the last few years. Yet the high-pressure electrodeless discharge, especially in a gas stream, is of great interest simply as a physical phenomenon, independently of its applied significance. In particular, it has become clear quite recently that the frequently employed term "plasma burner" reflects not only the outward similarity between the plasma flare of the plasmatron and the chemical flame of the ordinary burner. There is a deep physical and mathematical analogy between a discharge in a gas stream and the process of flame propagation in a combustible mixture[39].

We shall consider below the steady state of an already formed discharge. The questions of initial ignition, which are closely connected with the mechanism of high-frequency breakdown, will as a rule not be discussed.

II. EXPERIMENTS, CONSTRUCTIONS, APPLICATIONS

The ground work for modern research and applications of electrodeless discharges were laid immediately before the war by G. I. Babat at the "Svetlana" electric lamp factory in Leningrad. These researches were published in 1942[3] and became widely known abroad after being published in England in 1947[4]. Babat developed high-frequency vacuum tube oscillators with powers on the order of 100 kilowatts, which enabled him to obtain powerful electrodeless discharges in air at pressures up to atmospheric. Babat worked in the frequency range from 3 to 62 MHz, and the inductors consisted of several turns with a diameter on the order of 10 cm.

The high-frequency discharge was fed at a power that was tremendous for that time, up to several dozen kilowatts (incidentally, such values are high even for modern installations). Of course, it was impossible to "break down" air or any other gas at atmospheric pressure even by using the largest currents in the inductor, so that special measures had to be used to initiate the discharge. It was easiest to excite the discharge at low pressure, at which the breakdown fields were weak, and then gradually raise the pressure to atmospheric.

Babat noted that when gas flows through a discharge, the latter can be extinguished if the gas stream is too intense. At high pressures, a contraction effect was observed, i.e., a detachment of the discharge from the walls of the discharge chamber.

In the fifties, several articles were published on electrodeless discharges[5-7]. Cabannes[5] investigated discharges in inert gases at low pressures from 0.05 to 100 mm Hg and low powers up to 1 kW at frequencies 1–3 MHz, determined the ignition curves, measured the power input to the discharge by a calorimetric method, and measured the electron densities with the aid of probes. The ignition curves for many gases were also obtained in[7]. An attempt was made in[6] to use a discharge for ultraviolet spectroscopy.

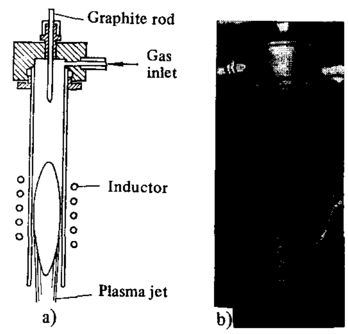

FIG. 2. Diagram (a) and photograph (b) of Reed's plasma burner [8].

An electrodeless plasma burner very similar to the present-day installations was constructed by Reed in 1960[8]. A diagram and photograph are shown in Fig. 2. A five-turn inductor made of copper tube, with spacing 0.78 cm between turns, is wound around a quartz tube of 2.6 cm diameter. The power supply was a commercial high-frequency generator with maximum output power 10 kW; the working frequency was 4 MHz. The discharge was ignited by a moving graphite rod. The rod, inserted into the inductor, was heated in the high-frequency field and emitted electrons. The surrounding gas became heated and expanded, and then broke down. After the ignition, the rod was removed and the discharge continued to burn.

The most important feature of this installation was the use of tangential gas inflow. Reed indicated that the produced plasma should propagate rapidly against the gas stream that tries to carry the plasma away. Otherwise, the discharge is extinguished, as is the situation with unstabilized flames. At low stream velocities, the plasma can be maintained by ordinary heat conduction. (The role of heat conduction in high-pressure discharge was noted also by Cabannes[5].) At large gas-supply velocities, however, it is necessary to employ measures for recirculating part of the plasma. A satisfactory solution of this problem was the vortical stabilization employed by Reed, in which the gas was fed into the tube tangentially and its motion through the tube was helical. Owing to the centrifugal outward motion of the gas, a reduced-pressure column is formed in the axial part of the tube. There is practically no axial flow, and part of the plasma is drawn upstream. The larger the supply velocity, the greater the penetration of the growing plasma upstream. In addition, at such a supply method the gas flows along the tube mainly near the walls, presses the discharge away from the walls, and insulates the walls from the destructive action of the high temperatures, making it possible to operate with higher pressures. These qualitative considerations, which were briefly formulated by Reed, are very important for the understanding of the phenomena, although they do not present a fully accurate picture of the nature of the phenomenon. In Ch. IV below we shall return to the problem of maintaining the plasma, which is the most serious in the case of a stationary stabilized discharge in a gas stream.

Reed operated with argon and with mixture of argon with helium, hydrogen, oxygen, and air. He noted that it is easiest to maintain the discharge in pure argon.

The argon flow was 10–20 liters/minutes (gas velocity averaged over the tube cross section 30–40 cm/sec) with the power introduced into the discharge 1.5–3 kW, amounting to approximately half the power drawn by the generator. Reed determined the energy balance in the plasmotron and measured by an optical method the spatial distribution of the temperature in the plasma.

He published a few more articles dealing with powerful inductive discharges at low pressures[9], with measurement of the heat transfer to the probes placed at various points of the plasma jet[10], and with the use of an induction burner for growing crystals of refractory materials[11].

An induction plasma burner similar in its construction to the Reed burner was described somewhat later by Reboux[45,46]. Reboux used this burner to grow crystals and to prepare small spherical samples of refractory materials.

Starting approximately in 1963, many Soviet and foreign papers have been devoted to experimental investigations of inductive high-pressure discharges in both closed vessels and in gas streams[12-33,40-44,53,60].

The spatial distributions of the temperature in the discharge region and in the plasma jet were measured, as well as the distributions of the electron densities. As a rule, known optical, spectral, and probe methods customarily employed in the investigation of arc-discharge plasmas have been used. The power fed to the discharge and the variations of the parameters were measured at different inductor voltages and different gas flows for different gases, frequencies, etc. It is difficult to establish some unified relationships, say, between the plasma temperature and the power fed to the discharge, since everything depends on the concrete conditions such as the tube diameter, the conductor geometry, the rate of gas supply, etc. The general result of many investigations is the conclusion that at a power on the order of several or a dozen kilowatts the temperature of the argon plasma reaches approximately 9000–10,000°K. The distribution of the temperature has in general a "plateau" at the center of the tube and drops off sharply near the walls, but the "plateau" is not quite flat, and in the central part there is a slight dip of approximately several hundred degrees.

In other gases the temperatures are also on the order of 10,000°, depending on the type of gas and other conditions. In air, the temperatures are lower than in argon at the same power, and conversely, to obtain the same temperatures the power required is several times larger[31]. The temperature increases slightly with increasing power and depends little on the gas flow. Figures 3 and 4 show by way of illustration the radial distributions of the temperature, the temperature field (isotherms), and the distributions of the electron densities. Experiments[27] have shown that with increasing rate and flow of the gas (in the case of tangential flow) the discharge becomes more and more detached from the walls and the radius of the discharge changes approximately from 0.8 to 0.4 of the tube radius. With increasing gas flow, the power fed to the discharge also decreases slightly, this being connected with the decrease of the discharge radius, i.e., of the plasma flow. In the case of discharges in closed vessels, without a continuous stream of gas, the glowing region of the discharge usually comes very close to the sidewalls of the vessel. Measurements of the electron densities have shown that the state of the plasma at atmospheric pressure is close to thermodynamic equilibrium. The measured concentrations and temperatures agree with satisfactory accuracy with the Saha equation.

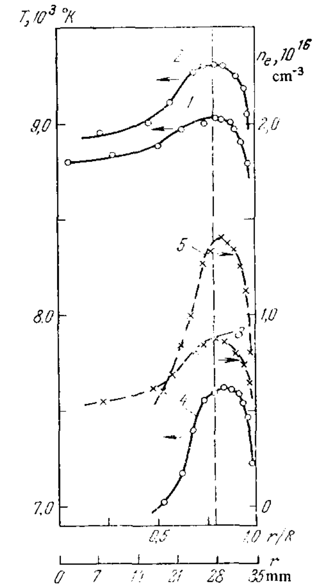

FIG. 3

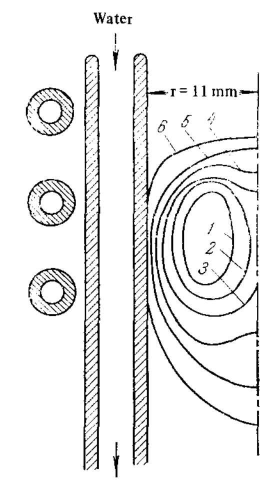

FIG. 4

FIG. 3. Radial distributions of the temperatures and of the electron densities as given in [24]. Discharge in an immobile plasma; tube radius 35 mm; frequency 11.5 MHz. 1, 2–temperatures T in argon at powers 4.7 and 7.2 kW; 3–electron density n_e in argon at 7.2 kW, 4, 5–T and n_e in xenon at 6 kW.

FIG. 4. Isotherms of argon discharge as given in [16]. Tube radius 11 mm; tube is cooled with water; frequency 26 MHz; power 2.5 kW; flow 80 cm³/sec. 1–T = 9750, 2–9650, 3–9400, 4–9000, 5–8700, 6–8400° K.

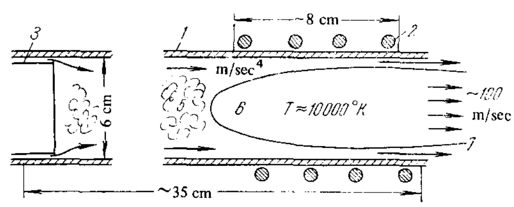

FIG. 5. Diagram of the plasmatron of the Institute of Mechanics Problems of the USSR Academy of Sciences IMP. 1–Tube, 2–inductor, 3–annular slit through which the gas is fed peripherally, 4–flow of cold gas, 5–turbulization region, 6–heated gas; 7–outgoing plasma jet.

We present data on a very recent installation developed by M. I. Yakushin at the Institute of Mechanics Problems of the USSR Academy of Sciences (IPM)[40]. Its diagram and main parameters are indicated in Fig. 5. Figure 6 shows a photograph of the discharge. The working gas is usually argon or air at atmospheric pressure. The inductor is fed from a high frequency vacuum-tube generator (LGD-30). The frequency range is 6–18 MHz. Owing to the improvements, it is possible to feed into the plasma up to 40 kW. The in-

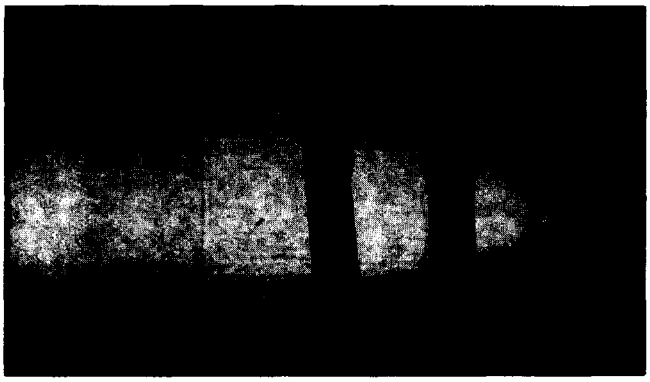

FIG. 6. Photographs of the discharge and of the plasma jet of the IPM plasmatron. Tube diameter 6 cm, air, power 27 kW, flow 2 × 10^3 cm^3/sec, temperature 9800° K.

ductor voltage is on the order of 5 kV. The gas is fed tangentially and flows through a quartz tube of 6 cm diameter and 35 cm.length. The flow is of the order of 10^2–10^3 cm^3/sec, and the axial velocity averaged over the cross section is on the order of several dozen centimeters or one meter per second. The axial velocity decreases rapidly in the axial direction with increasing distance from the tube wall. The discharge radius is 0.4–0.8 of the tube radius. We present two examples of the parameters: 1) air, flow 1.3 × 10^3 cm^3/sec, average velocity 55 cm/sec, power 21.3 kW, maximum radius of the discharge region 0.69 of the tube radius, "plateau" temperature 9700°K; 2) argon, flow 2.1 × 10^3 cm^3/sec, velocity 90 cm/sec, power 5.5 kW, ratio of the radii 0.7, "plateau" temperature 8000–8200°K.

We note a few other applications of the induction discharge and of the plasmatron, besides those indicated above. The discharge was used to heat gas in a supersonic aerodynamic low-density tube[54] in order to feed additional energy to a plasma jet obtained from an arc plasmatron[55], so as to increase the per-unit momentum in electrothermic motors and to improve the distribution of the flow parameters. The plasma jet was used to investigate the effect of high temperatures and heat flux on different materials, to stimulate conditions under which the heat-insulating coatings of flying craft operate[56,57]. Microwave plasmotrons have also been developed[58,59]. In the installation of[59], gas flows through a tube that passes through a waveguide. A discharge is maintained at the point of intersection as a result of the microwave absorption, and a plasma jet flows out of the tube. Microwave plasmotrons are beyond the scope of the present article.

We now proceed to a theoretical analysis of the inductive discharge. More detailed data on applications and certain experiments can be found in the review articles[52], where there is also a complete bibliography on high-frequency discharges and their applications.

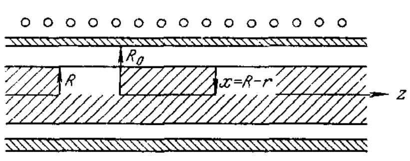

FIG. 7. Diagram of static discharge.

III. DISCHARGE IN AN IMMOBILE PLASMA

The state of the stationary static discharge regime in an immobile plasma makes it possible to explain the important features of the discharge in a stream. In almost all papers, it is the static process that is considered. The problem is as a rule idealized, namely, the solenoid is assumed to be infinitely long, i.e., the process is assumed to be one-dimensional. The stationarity of the process is ensured by dissipating the heat released by drawing away the heat released in the wall of the cooled dielectric tube (radius R_0; Fig. 7). The principal problem of the theory in this case is to calculate the plasma temperature, the power input to the discharge, and the electrotechnical parameters of the discharge, namely the ohmic resistance and the inductance, as functions of the current in the solenoid.

Once these relations are established, it is easy to change over to a representation using some other (arbitrarily chosen) primary quantity, for example, the power.

1. "Metallic Cylinder" Model

In the simplest model, which describes the electrodynamic aspect of the process fairly well, the plasma column is likened to a metallic cylinder with constant conductivity σ and radius R. The gas in the gap between the solenoid and the conductor, i.e., at $R < r < R_0$, is assumed to be nonconducting. Estimates based on such a model were obtained by many, starting with Thomson[2]. The electromagnetic field satisfies Maxwell's equations in which the displacement currents can be neglected under the frequencies employed in practice:

$$\operatorname{rot} \mathbf{H} = \frac{4\pi}{c}\sigma \mathbf{E}, \quad \operatorname{rot} \mathbf{E} = -\frac{1}{c}\frac{\partial \mathbf{H}}{\partial t} \tag{1}$$

(we assume here $\mu = 1$). Bearing in mind that **H** and **E** are proportional to $\exp(-i\omega t)$, and taking it into account that the magnetic field has only an axial component and the electric field only an azimuthal component, we obtain for the complex amplitudes $H = H_z$ and $E = E_\varphi$ the equations

$$-\frac{\partial H}{\partial r} = \frac{4\pi}{c}\sigma E, \quad \frac{1}{r}\frac{\partial}{\partial r} rE = \frac{i\omega H}{c}. \tag{2}$$

In the nonconducting gap, the amplitude of the magnetic field is constant and is determined by the ampere turns of the solenoid:

$$H_0 = 4\pi In/c; \tag{3}$$

here I is the amplitude of the current in the solenoid in absolute units, and n is the number of turns per unit length; the time reference can always be chosen such as to make H_0 real.

The solution of the system (2) in a conductor should satisfy the condition that it be finite on the axis at $r = 0$ and that $H = H_0$ at $r = R$. The solution is expressed in terms of Bessel functions of the first kind (see, for example[27]):

$$H = H_0 J_0(kr)/J_0(kR),\quad E = H_0(\omega/8\pi\sigma)^{1/2}(1+i)J_1(kr)/J_0(kR), \tag{4}$$

where

$$k = (2i)^{1/2}/\delta = (1+i)/\delta,$$

and

$$\delta = c(2\pi\sigma\omega)^{-1/2} = 5.03/[\sigma(\Omega^{-1}\text{cm}^{-1})\,\nu(\text{MHz})]\ \text{cm} \tag{5}$$

is the thickness of the skin layer, i.e., the effective depth of penetration of the field into the conductor.

The Bessel functions contained in these formulas, which have a complex argument of the type $z\sqrt{i}$ ($z = \sqrt{2}r/\delta$), are calculated with the aid of the tabulated Kelvin functions[48] $J_0(z\sqrt{i}) = \text{ber}\, z - i\,\text{bei}\, z$. The radial distributions of the field amplitudes are shown in Fig. 8.

The power of the Joule loss in the conductor (the power input to the "plasma") is

$$W = \int_0^R \sigma\langle E^2\rangle\cdot 2\pi r\,dr \tag{6}$$

per unit length of the cylinder; the symbol $\langle\ldots\rangle$ denotes the operation of averaging of the oscillating quantities over the period of the field oscillations. By using known transformation[47], it is possible to express the power in terms of the flux of electromagnetic energy into the conductor, i.e., in terms of the fields on the surface:

$$W = 2\pi R\,|S_R|,\quad S_R = c\langle[\mathbf{EH}]\rangle_{r=R}/4\pi. \tag{7}^*$$

All the formulas become particularly simple in that limiting case of practical importance when the thickness of the skin layer is small compared with the radius, $\delta \ll R$. The thin layer of the conductor, in which the field penetrates, is then essentially flat and it is possible to consider the planar problem in place of the cylindrical problem[47]. Of course similar results are obtained also from the general formulas (4) and (7) by changing over in them to the asymptotic representations of the Bessel functions at large values of the argument. Let x be the coordinate reckoned from the plane surface inside the conductor ($x = R - r$; see Fig. 7). The amplitudes of the fields H and E decrease with increasing depth inside the body like $\exp(-x/\delta)$, and the electromagnetic flux density entering into the conductor, i.e., the power per unit surface, is

$$S_0 = (cH_0^2/16\pi)(\nu/\sigma)^{1/2} = 3.16\cdot 10^{-2}(In)^2\,(\text{A-V/cm})\,[\nu(\text{MHz})/\sigma(\Omega^{-1}\text{cm}^{-1})]^{1/2}\ \text{W/cm}^2 \tag{8}$$

Another very simple limiting case is that of weak screening of the field by the conductor: $\delta \gg R$. Then $H \approx H_0$,

$$E \approx i\omega H_0 r/2c$$

and

$$W = (\pi\sigma\omega^2 H_0^2 R^4/16c^2) = \pi^3\sigma\omega^2(In)^2R^4/c^4. \tag{9}$$

In the general case, at an arbitrary ratio of R and δ, it is convenient to represent $|S_R|$ and W in the form

$$|S_R| = S_0 f,\quad W = 2\pi R\,|S_R| = 2\pi R S_0 f, \tag{10}$$

and calculation by means of formulas (7) and (5) shows that the factor f depends only on the ratio R/δ and equals[49].

$$f = \sqrt{2}\,(\text{ber}\,\alpha\cdot\text{ber}'\,\alpha + \text{bei}\,\alpha\cdot\text{bei}'\,\alpha)/(\text{ber}^2\alpha + \text{bei}^2\alpha),\quad \alpha = \sqrt{2}R/\delta.$$

The function $f(\alpha)$ is shown in Fig. 9.

In order to apply formulas (10) and (8) to a discharge, it is necessary to know the conductivity σ and the radius R. They are specified in practice in the same manner as the plasma column temperature T_m is specified, since at the high gas density corresponding to atmospheric pressure and to a temperature $T \approx 10^4\,^\circ$K, the deviations from the thermodynamic equilibrium are fortunately small, and the conductivity is therefore simply a function of the temperature (and of the pressure). The functions $\sigma(T)$ at p = 1 atm. for argon and air are shown in Fig. 10. As seen from the plots, at temperatures below 7000–8000°K the conductivity decreases very sharply with decreasing temperature (roughly speaking, in proportion to the electron

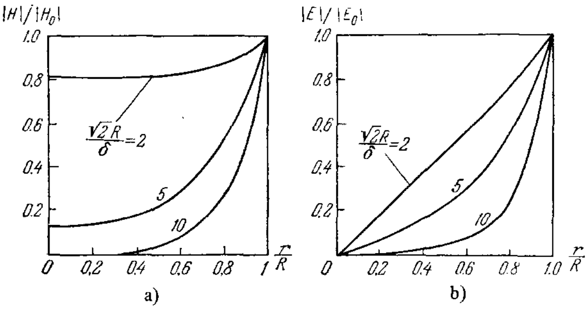

FIG. 8. Distributions of the moduli of the field amplitudes along the radius at different ratios of the conductor radius to the skin-layer thickness.

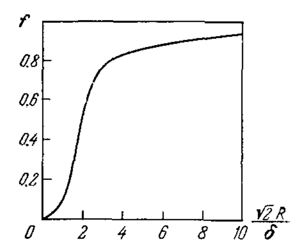

FIG. 9. The function $f(\sqrt{2}\,R/\delta)$.

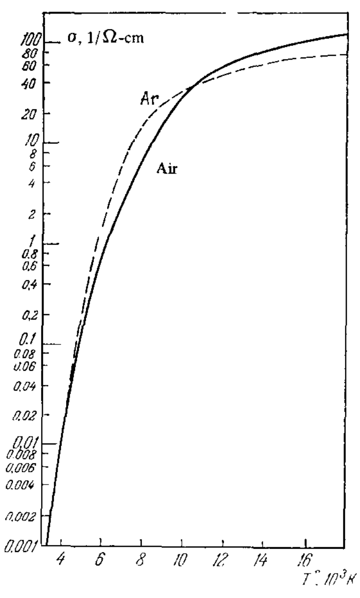

FIG. 10. Electric conductivities of air and argon at atmospheric pressure.

---
*$[\mathbf{EH}] \equiv \mathbf{E}\times\mathbf{H}$.

density, i.e., $\sim \exp(-I_i/2kT)$, where I_i is the gas ionization potential). Therefore the temperature boundary of the discharge, meaning also the radial boundary, should be quite abrupt. By discharge boundary we mean here the boundary that separates effectively the weakly conducting gas, in which there is practically no heat release and which screens the magnetic field weakly, from the gas with relatively high conductivity, where the Joule heat is released.

Under conditions when the gas is immobile and the energy released in the discharge is carried away by heat conduction in the tube walls, this boundary is established at a radius such that the temperature gradient produced in the gap between the plasma and the walls is precisely such as to ensure the heat transfer to the wall. It is easy to write the corresponding equation for R[20,33].

The heat flux, by virtue of the axial symmetry, is directed along the radius and is equal to

$$\mathcal{J} = -\varkappa(T)\, dT/dr, \tag{11}$$

where $\kappa(T)$ is the thermal conductivity coefficient. The stationary equation of thermal conductivity in the region $R < r < R_0$, where there are practically no sources ($\operatorname{div}\mathcal{J} = 0$) can be directly integrated and yields, together with the obvious conditions $T(R) = T_m$, $\mathcal{J}(R) = |S_R|$, and $T(R_0) = T_W \approx 0$,

$$\int_{T_w \approx 0}^{T_m} \varkappa(T)\, dT = \frac{W}{2\pi} \ln\left(\frac{R_0}{R}\right) \approx (R_0 - R) \frac{W}{2\pi R_0} \tag{12}$$

(the wall temperature is $T_W \ll T_m$ and can be set equal to zero).

The last simplification in (12) is valid if the discharge boundary, as is most frequently the case, lies close to the wall and $R \approx R_0$. It is easy to see that the radius of the stationary discharge is stable. Indeed, if the discharge approaches the wall for some reason, other conditions remaining the same, the temperature gradient increases, the heat transfer to the wall becomes larger than the heat released, the layer next to the wall becomes cooler, and the boundary moves away (and vice versa).

2. More Detailed Calculations and Plasma Temperature

The question of the temperature or the conductivity of the plasma cannot be solved within the framework of the purely electrodynamic theory of the "metallic cylinder." In estimating the power by means of formulas (10) and (12), it is necessary to specify in some manner the value of σ, because the temperature and the conductivity of the plasma are determined in fact by the energy balance in the discharge region itself.

The problem of a discharge in an infinite solenoid was first formulated rigorously by Soshnikov and Trekhov[34]. Inasmuch as the conductivity of the gas in the tube is a function of the temperature, and the radial distribution of the temperature is regulated by the thermal conductivity, the electrodynamic equations (2) must be supplemented by the heat-conduction equation with heat sources. In the stationary case

$$\operatorname{div}\mathcal{J} = r^{-1}\, d(r\mathcal{J})/dr = \sigma\langle \mathbf{E}^2\rangle - \varphi(T), \tag{13}$$

where the term $\varphi(T)$ describes the thermal-radiation energy loss, account of which was taken in[34]. The solution of the system (2), (11), and (13), for the functions H, E. T, and $\mathcal{J}$ should satisfy the corresponding boundary conditions. On the axis at $r = 0$ we have $\mathcal{J} = 0$ and $E = 0$. At the internal surface of the tube at $r = R_0$, the magnetic field is determined by the ampere turns, $H = H_0 = 4\pi\, \mathrm{In}/c$, and the heat flux and the temperature satisfy the condition of heat transfer to the walls; it is possible, for example, to put simply $T = T_W \approx 0$.

In[34-36], the equations were integrated numerically. Naturally, their number has increased by two, since the real and imaginary parts of the complex amplitudes H and E are independent functions. A numerical solution of the system with boundary conditions imposed at the different limits of the integration region entails certain difficulties, so that in[34-36], they solved, as it were, the inverse problem. In fact, the initially specified parameters should be the ampere turns of the solenoid and the tube radius, H_0 and R_0. The solution should yield the temperature and the magnetic field on the axis, $T(0)$ and $H(0)$, and by virtue of the uniqueness of the solution there is a correspondence between the pairs of quantities H_0, R_0, and $T(0)$, $H(0)$. To simplify the calculation, the authors of[34-36] specified $T(0)$ and $H(0)$ in lieu of H_0 and R_0, making it possible to start the integration of the equations from the point $r = 0$. At a certain radius, the temperature decreases very sharply. The radius corresponding to $T \approx 0$ was taken to be R_0, and the number of ampere turns was determined from the absolute magnitudes of the magnetic fields at that point, using formula (3). The power was calculated by formula (6)*. The described procedure is perfectly correct in principle, but of course has the shortcoming that it is necessary to guess the values of $T(0)$ and $H(0)$ in order to arrive at the desired parameters H_0 and R_0 corresponding to the experiment. In[34-36] they calculated many variants for air and argon at several frequencies, temperatures, and fields on the axis. Figure 11 shows by way of illustration the obtained radial distributions and the corresponding calculated parameters. The characteristic small temperature drop in the region of the axis is the consequence of the radiation loss: the loss is volume-dependent, but the heat release occurs mainly in the peripheral layer, and therefore the central region becomes cooled somewhat compared with the peripheral region. Calculations have shown that at temperatures above 10,000–12,000°, the radiation loss becomes quite appreciable, and at lower temperatures the loss is small.

By replacing the $T(r)$ curves in Fig. 11 by equivalent "steps" it is easy to choose in each case the effective values of R and $\sigma(T_m)$ for the "metallic rod" model. Indeed, the power estimated by formulas (9) and (8) turn out to be quite close to the calculated power.

To determine the main regularities of the inductive discharge, it is very important to establish what de-

*Knowing the distribution of the fields and the conductivity, it is easy to calculate the inductance and the ohmic resistance of the discharge.

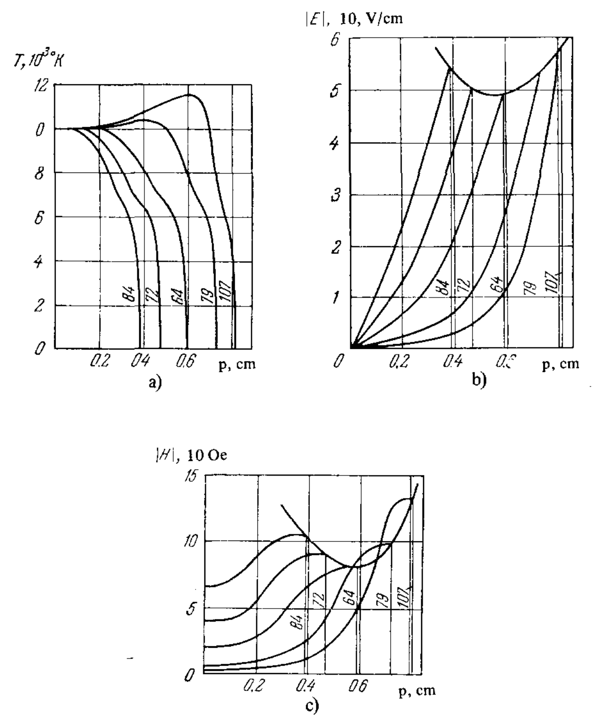

FIG. 11. Radial distribution of the temperature and of the field amplitudes [34]. Static discharge in air, frequency 50 MHz. The number of ampere turns per centimeter is marked on each curve. For the set of numbers 84, 72, 64, 79, 107 the energy release amounts to 2.0, 2.4, 2.8, 5.1, and 10.5 kW/cm, and the radiation loss is 0.03, 0.05, 0.09, 0.35, and 2.0 kW/cm, respectively.

termines physically the plasma temperature, and how this temperature depends on the magnitude and frequency of the current in the inductor, on the tube radius, and on the properties of the gas. This question was first solved by Gruzdev, Rovinskiĭ and Sobolev[37], who considered the problem in the same initial formulation as in[34-36] (but without allowance for the radiation loss). We omit the energy balance equation (13) the loss term $\varphi(T)$ and use the Maxwell's equations (1) to rewrite it in a divergence form

$$\operatorname{div}(\mathcal{J}+\mathbf{S})=0, \quad \mathbf{S}=c\langle[\mathbf{EH}]\rangle/4\pi. \tag{14}$$

This yields immediately the first integral of the system—the integral of conservation of the total energy flux. With allowance for the boundary conditions on the axis, the sum of the fluxes along the radius is equal to zero:

$$\mathcal{J}+S=0, \tag{15}$$

i.e., the flux of electromagnetic energy from the solenoid, to the axis ($S<0$) is cancelled out at each point by the heat flux going in the direction of the wall (in the absence of radiation loss we have throughout $\mathcal{T}>0$). It turns out that the system (1), (11), and (14) has also a second integral. We eliminate E from the expression (14) for the Poynting vector, using the first equation of (1). We obtain

$$S=(c/4\pi)\,|\langle[\mathbf{EH}]\rangle|=-(c^2/32\pi^2\sigma)\langle dH^2/dr\rangle=-(c^2/64\pi^2\sigma)\,d\,|\mathrm{H}|^2/dr, \tag{16}$$

where $|\mathrm{H}|$ is the real amplitude of the oscillating magnetic field. Substituting expressions (11) and (16) in (15), multiplying everything by σ, and integrating the resultant equation with allowance for the boundary conditions at the tube, where $T\approx 0$ and $H=H_0$, we obtain the second integral of this system:

$$\int_0^{T(r)}\sigma(T)\varkappa(T)\,dT=\frac{c^2H_0^2}{64\pi^2}\left[1-\frac{|H(r)|^2}{H_0^2}\right]. \tag{17}$$

Referring Eq. (17) to the point $r=0$ and taking (3) into account, we obtain an equation that determines the temperature on the axis, i.e., the maximum plasma temperature T_m:

$$\int_0^{T_m}\sigma(T)\varkappa(T)\,dT=\left(\frac{In}{2}\right)^2\left[1-\frac{|H(0)|^2}{H_0^2}\right]. \tag{18}$$

In the first approximation we can obtain the temperature T_m (and incidentally all the distributions $T(r)$) by substituting in (17) and (18) the values of $|H(r)|$ and $|H(0)|$ in accordance with formula (4) for the "metallic cylinder." The constants σ and R must be taken to be $\sigma=\sigma(T_m)$ and R_0. This yields the equation

$$\int_0^{T_m}\sigma\varkappa\,dT=\left(\frac{In}{2}\right)^2\left[1-\frac{1}{\operatorname{ber}^2(\sqrt{2}R_0/\delta)+\operatorname{bei}^2(\sqrt{2}R_0/\delta)}\right], \tag{19}$$

where δ is determined by formula (5). Equation (19) allows us to calculate approximately T_m as a function of In, ω, and R_0 for any gas. The equation simplifies strongly in the limiting cases of strong and weak screening of the magnetic field by the plasma.

In the case of a thin skin layer, $\delta \ll R$ (high temperatures, high frequencies), which are of greatest practical interest, we have $|H(0)| \ll H_0$ and

$$\int_0^{T_m}\sigma(T)\varkappa(T)\,dT=\left(\frac{In}{2}\right)^2, \tag{20}$$

i.e., the plasma temperature does not depend on the frequency and on the radius of the tube and is determined only by the number of ampere turns and the properties of the gas. This important conclusion of the theory is confirmed by experiment. Equation (20) does not hold for the case of very many ampere turns and very high temperatures, higher than 13,000–15,000°, when the radiation loss becomes an appreciable fraction of the power input, and the temperature has a strong peak on the periphery, as follows from the calculations of[34-36]. In modern installations, however, the temperatures do not exceed approximately 10,000°, and the conclusions of this theory are unconditionally valid in this case. In the upper limiting case of weak screening, $\delta \gg R$ (low temperatures, low frequencies), we have

$$\int_0^{T_m}\sigma\varkappa\,dT=\left(\frac{In}{2}\right)^2\frac{\pi^2\omega^2R_0^4\,[\sigma(T_m)]^2}{c^4}. \tag{21}$$

After calculating T_m, i.e., $\sigma=\sigma(T_m)$, we can determine the power by means of formulas (8)–(10) and (12) of the "metallic cylinder" model, and estimate the effective discharge radius R. In[37] the calculations were made also in the second approximation, but the resultant equations are very cumbersome. In the same paper, corrections were also derived to account for the finite length of the inductor and estimates of the tube heating.

In Table I, taken from[37], are listed the results of the calculation of the temperature, power, and optimal

Table I

T_m, 10^3 °K	In, A-V/cm	W, kW/cm	$r(4500°\ K)/R_0$
8.0	13.3	0.21	0.907
8.5	17.7	0.36	0.948
9.0	22.6	0.54	0.964
10.0	33.0	1.06	0.983
10.5	39.2	1.43	0.987

radius of the point at which T = 4500°K for argon at p = 1 atm., R_0 = 3.75 cm, ν = 12 MHz and several values of the ampere turns. In all these variants, $\delta \ll R$.

The calculation results are in fair agreement with the experimental data.

Equations (19)—(21) for the temperature, together with expressions (6), (8), and (10) for the power, making it possible to determine the connection between the power, the ampere turns, and the temperature. This is done in[38], where the optimal frequency range, from the point of view of obtaining a specified plasma temperature T_m, is determined for the discharge. Figure 12, taken from that paper, shows the variation of the power and the ampere turns with the variation of the parameter $\beta = 2R^2/\delta^2$, which is proportional to the frequency (see formula (3)). It is seen from Fig. 12 that since it is natural to attempt to reduce the power loss and to decrease the current in the inductor, it is meaningless to go beyond the range $10 < \beta < 30$, corresponding to the ranges $0.25 < \delta/R < 0.45$ and $125 < \nu(\mathrm{MHz})/\sigma(\mathrm{ohm}^{-1}\,\mathrm{cm}^{-1})R\,(\mathrm{cm}) < 380$.

Formulas (20) and (8) lead also to the natural conclusion that the power necessary to reach a given temperature T_m increases quite rapidly with increasing temperature[38]. At T > 10,000—12,000°, when the resistance is determined by the Coulomb collisions of the electrons with the ions, we have $\sigma \sim T^{3/2}$. The total conductivity also increases with the temperature, and roughly $W \sim T^{\gamma}$, where $\gamma \approx 2.5$—3. It should be noted, however, that the required power increases rapidly also as a result of the increasing radiation loss. It is not clear which of the two factors plays the decisive role. There are still no calculations that make it possible to estimate directly the comparative role of the two main causes of the rapid increase of power with increasing temperature at high temperatures.

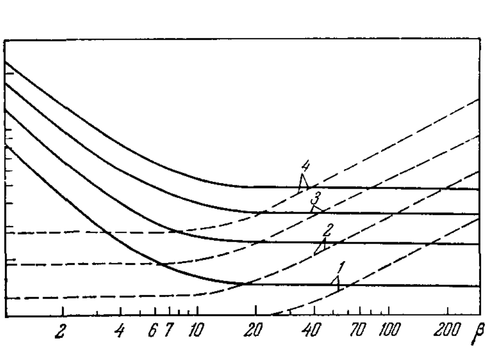

FIG. 12. Qualitative dependence of the ampere terms per centimeter (solid line) and of the power per centimeter of inductor length (dashed lines) on $\beta = (\sqrt{2}\,R_0/\delta)^2$ at several fixed temperatures [38]: 1—T = 8000, 2—9,000, 3—10,000, 4—11,000° K.

Freeman and Chase[33] analyzed the discharge on the basis of the "metallic cylinder" model. Assuming the ampere turns (i.e., H_0) and the tube radius R_0 to be specified, the authors write out expression (10) for the power as well as Eq. (12). The latter has the meaning of the radius of the stationary discharge, at which the thermal conductivity in the "gap" precisely ensures the transfer of the heat due to the power released to the tube walls. We have seen above that the third missing equation, which determines essentially the unknown conductivity of the "metallic cylinder," follows from an analysis of the energy balance in the plasma itself. However, Freeman and Chase use instead an equation expressing the condition of the minimum of the power at specified H_0 and R_0, justifying this operation by rather nebulous considerations concerning the minimum of "entropy production." In their opinion, the plasma in the discharge is heated to such a temperature at which the minimum power is consumed in the maintenance of the stationary discharge, given the current in the solenoid, the radius of the tube, and the heat-transfer conditions.

We see no physical grounds for such an assumption, and the result of this assumption is also strange and contradicts the experimental data. Namely, it follows from the minimum condition that a discharge with a skin layer δ smaller than 0.57 of the discharge radius cannot exist. Yet in most experiments the skin layer, to the contrary, is thin and a splendid discharge is produced. The situation is apparently different. It is necessary to assume that the minimum condition corresponds to some degree to the optimal conditions for the discharge. We mentioned above the optimal frequency, other conditions being equal. Consequently, at a given frequency there exists also an optimal temperature or conductivity. This apparently explains the agreement between the theory of Freeman and Chase with their own experiments. The question is not yet completely clear and calls for a special analysis. At any rate, the minimum condition cannot replace in any way the connection between the temperature and the ampere turn (established in[37]), which is the consequence of exact equations of the discharge, is subject to no doubt, and furthermore admits of the existence of regimes with thin skin layers.

IV. STATIONARY DISCHARGE IN A GAS STREAM

An inductor discharge in a gas stream, i.e., the process actually occurring in the electrodeless plasmatron, were considered theoretically in three papers[12,39,50]. The first of them[12] is among the early papers on plasma burners; it describes experiments and attempts to present a general quantitative analysis of the phenomenon, but the small section of the paper dealing with the discharge in a stream and the hydrodynamic aspect of the problem is based on incorrect premises. Nor is it possible to agree with certain fundamental premises of the third article[50]. However, the results of the calculations presented in it, if regarded from correct points of view, are quite interesting and instructive. The results or[12,50] will be considered in Sec. 4 below, after we become acquainted with the evolution of the discharge process in a stream. The present chapter is based on the concepts developed in[39].

1. Quantitative Picture and Analogy with Flame Propagation

We shall consider the process that occurs in a plasma burner of the Reed type[8], with helical flow of the gas in the tube.

For concreteness, the numerical estimates and calculations will pertain to the parameters of the setup of our institute (IMP), referred to at the end of Ch. II.

Let us consider a stationary burning discharge. In order for induced currents to flow in the gas, it is necessary that the gas entering the discharge region be sufficiently ionized, i.e., already highly heated. It was established already in earlier investigations that the gas is heated by conduction from the previously heated layers. In this respect, the process is analogous to slow combustion, in which the heat of the combustible mixture to the ignition temperature is obtained by heat conduction. Another mechanism of preparing the mixture for ignition is the diffusion of the active reagents from the flame. In this case the analog is the diffusion of electrons. However, the diffusion is ambipolar and is slower than the heat transfer, owing to the smallness of the diffusion of the ions compared with the diffusion of the neutral particles.

Just like the rate of a chemical reaction, electric conductivity increases with increasing temperature, and especially sharply at temperatures below 8,000°K. Therefore, in the case of a discharge it is also appropriate to speak of an "ignition" temperature, namely the ionization temperature T_0, defined as a quantity such that when $T < T_0$ the gas is practically nonconducting and screens the electric field weakly, and at $T > T_0$ the Joule heat of the induction currents is released in the gas and the magnetic field is attenuated. The surface having the temperature T_0 can be called arbitrarily the discharge front.

The discharge (energy release) occurs in a certain annular layer inside the inductor. The effective width of the discharge ring a, equal to half the thickness of the skin layer δ for the penetration of the magnetic field, is in many practical cases rather small compared with the radius. Thus, for example in air and atmospheric pressure and $T = 10{,}000°$ we have $\sigma = 25\ \text{ohm}^{-1}\ \text{cm}^{-1} = 2.2 \times 10^{13}\ \text{sec}^{-1}$, and at a frequency $\nu = 15$ MHz we have $a = \delta/2 = 0.15$ cm (see formula (5)), whereas the radius of the discharge is $R \approx 2$ cm.

The thickness Δ of the heated layer in front of the discharge is several times larger than a. The zones of the discharge ("chemical reaction") and heating, which together form the "flame," are shown cross hatched in Fig. 13, which illustrates the general scheme of the process as treated in this theory. The figure shows also the gas streamlines, or more accurately the projections of the helical lines on the plane of the diametral cross section. The streamlines are refracted in the "flame," since the heated gas expands and is accelerated principally in a direction perpendicular to the surface. The internal cavity of the discharge ring is filled with gas ("combustion products") heated to the final temperature T_f.

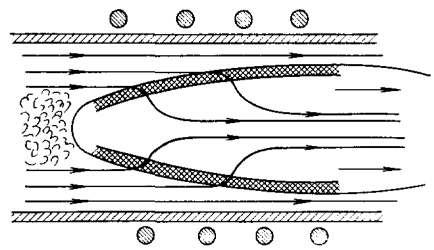

FIG. 13. Qualitative scheme of the process in accordance with the concepts of [39]. The "flame" is shown doubly cross-hatched.

The convergence of the gas stream to the axis leads to a certain increase of the pressure in the axial region inside the inductor, and it is possible that part of the heated gas is drawn from there upstream into the vortical zone with decreased pressure. This apparently produces the hot-gas recirculation noticed by Reed[8]. In the case of large gas flows, a high-temperature tongue is produced and penetrates far forward in a direction opposite to the cold gas. We note that all the velocities here are subsonic and the pressure drops are small.

The most important feature of the process is that the lateral front of the discharge is inclined relative to the incoming gas streams in such a way, that the cold gas, just as in combustion, enters the "flame" in a normal direction with a perfectly defined velocity. In analogy with combustion theory[51], we shall call this the normal discharge propagation velocity u. As will be shown below, $u \sim 10$ cm/sec and therefore the angle of inclindation of the front is small at axial gas velocities $v \sim 1$ m/sec.

At the same time it is clear (and important) that the lateral front of the discharge can never become strictly parallel to the gas stream that presses it away from the two walls, and the gas must penetrate in the discharge from the lateral surface. In fact, let us imagine for an instant that the surface of the front is parallel to the stream. The heat propagates in the radial direction and as soon as the gas is heated to the ionization temperature T_0, the front of the discharge goes over to a new place. But since the heat is still carried away by the stream, it propagates farthest along the radius in the rear part of the inductor, where gas particles heated by the passage of the front part enter. Therefore the isotherm T_0 becomes inclined to the stream and the stationary state is established precisely when the heat loss is exactly offset by the heat supply. This occurs when the increasing velocity of gas influx into the discharge in the normal direction reaches the value u.

It should be noted that in addition to a similarity, there is also an appreciable difference between an electrodeless discharge in a stream and combustion. In the absence of energy loss, the final temperature of the combustion products does not depend on the flame propagation conditions and is determined only by the heat-production ability of the mixture. In a discharge, the final temperature depends on external conditions even at a specified rate of supply of electromagnetic energy, and actually the power itself is unknown.

The main purpose of the theory of a discharge in a stream is to calculate the final temperature and the power fed into the discharge (just as in the case of the static process), as well as the flow of the gas heated to the high temperature; the latter is already a new feature compared with the static regime.

2. The Problem of Normal Discharge Propagation

To construct a quantitative theory it is natural to use the procedure employed in combustion theory, where the first step is to determine the normal propagation of the flame and to calculate the fundamental quantity, namely the normal flame propagation velocity, and only then are flames of different configurations considered. It must be emphasized that the analogy between the discharge in a stream and the propagation of a flame helps understand the physics of the process, makes it possible to examine the discharge in a stream from a different point of view, which reveals unexpected features of the phenomenon, and suggests an effective way of constructing the theory, but does not serve in any way as the basis of the theory. The theory can be developed with equal success in the same form without resorting to the analogy.

Thus, let us consider the idealized problem of normal discharge propagation. We focus our attention on some section of the "flame" (Figs. 13 and 14) and make some simplifying assumptions. Using the fact that the layer is relatively thin, we shall assume it to be plane and one-dimensional, i.e., having no gradients along the surface. In setting up the equations of the electromagnetic field, we neglect the inclination of the discharge front to the inductor axis and assume the inductor to be an infinite solenoid. Then the vectors H and E are tangent to the surface. We neglect, further, the energy loss to radiation $\varphi(T)$ and a certain outflow of heat into those cold-gas layers which only push the discharge away from the tube walls but do not fall themselves into the discharge. We emphasize that the diversion of the heat from the energy-release zone into those cold-gas layers which subsequently fall into the discharge is not a loss, since the heat remains in the plasma.

We direct the x axis perpendicular to the surface of the discharge in the interior of the layer, where the energy release takes place (see Fig. 14). The tangential component of the velocity of the incoming oblique gas stream remains practically unchanged, owing to the smallness of the gradient along the surface, and the normal component v_x changes in accordance with the continuity equation $\rho v_x = \rho_0 u$, where ρ_0 is the density of the cold gas. The density $\rho(x)$ decreases with increasing temperature $T(x)$, roughly speaking, like $1/T$, since the pressure remains approximately constant*.

Let us write down the energy equation, bearing in mind that in the stationary process we have for a gas particle $dT/dt = v_x dT/dx$:

$$\rho_0 u c_p dT/dx = -(d\mathcal{J}/dx) + \sigma\langle E^2\rangle, \quad \mathcal{J} = -\varkappa\, dT/dx; \tag{22}$$

Here c_p is the specific heat of the gas of constant

*The pressure drop across the layer is small; the magnetic pressure is even smaller than the gas-pressure drop and does not play any role.

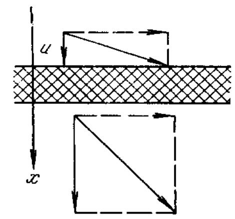

FIG. 14. Section of the "flame" layer The resolution of the velocities shows the cause of the refraction of the stream lines.

pressure; Eq. (22) is a generalization of Eq. (13). Maxwell's equations (2) in the planar case ($H = H_z$ as before; E_φ is now replaced by $E_y = E$) take the form

$$-dH/dx = 4\pi\sigma E/c, \quad dE/dx = i\omega H/c. \tag{23}$$

The boundary conditions for the system (22) and (23), which describes the process in the layer under consideration, follow, just as in the static case, from the physical formulation of the problem. The field does not penetrate in the interior of the conducting plasma, where the temperature assumes a certain constant final value T_f, i.e., the heat flux also vanishes. Sufficiently far in front of the discharge, the gas is cold, i.e., $T_\infty \ll T_f$, the heat flux is completely absorbed and lost, and the magnetic field is determined by the ampere turns of the inductor in accordance with formula (3). Thus, the solution of the system of four equations of first order for the functions H, E, T, and $\mathcal{J}$ should satisfy the five boundary conditions:

$$\left.\begin{array}{ll} \text{at} & x = +\infty \quad \mathcal{J} = 0, \quad H = 0, \\ \text{at} & x = -\infty \quad \mathcal{J} = 0, \quad T = T_{-\infty} \approx 0, \\ & \qquad H = H_0 = 4\pi I n/c. \end{array}\right\} \tag{24}$$

This is possible only at a chosen value of the propagation velocity u, which enters into the system in the form of an unknown parameter and must be determined by solving the equations—a situation analogous to that occurring in the theory of flame propagation.

The system (22)–(24) has an integral that reflects the condition of the conservation of the total energy flux. Indeed, integrating (22) from $-\infty$ to x with the aid of (23) and (24), we obtain an equation generalizing (15):

$$\rho_0 u w + \mathcal{J} + S = S_{-\infty}, \tag{25}$$

$$w = \int_0^T c_p\, dT, \quad S = \frac{c}{4\pi}\langle EH\rangle = -\frac{c^2}{32\pi^2}\frac{1}{\sigma}\left\langle\frac{dH^2}{dx}\right\rangle; \tag{26}$$

Here w is the specific enthalpy of the gas, S is as before the density flux of the electromagnetic energy; $S_{-\infty}$ pertains to the point $x = -\infty$ and represents the electromagnetic power that is received from the solenoid per unit discharge surface. Referring Eq. (25) to the point $x = +\infty$, we obtain the energy balanced equation for the layer

$$\rho_0 u w_f = S_{-\infty}, \quad w_f = w(T_f). \tag{27}$$

This trivial equation connects the unknown quantities u, W_f, and $S_{-\infty}$, which are to be determined. With the aid of (27), the integral (25) can be rewritten in the form

$$\mathcal{J} = \rho_0 u (w_f - w) - S. \tag{28}$$

After solving this problem, the power P delivered to the discharge and the flow G of the gas to be heated are determined from

$$P = \int S_{-\infty}\,dF, \quad G = \int u\,dF, \tag{29}$$

where the integration is over the outer surface of the discharge.

It is possible to obtain an approximate solution of the system of equations by using a method that corresponds to a known degree to the "metallic cylinder" model, namely, the true distribution of the conductivity $\sigma(x)$, which is shown in Fig. 15 together with the temperature distribution $T(x)$, is replaced by a step function: $\sigma = 0$ when $x < 0$ and $\sigma = \text{const}$ when $x > 0$. As seen from the figure, where the approximated step function $\sigma(x)$ is shown dashed, the constant conductivity corresponds to the final plasma temperature: $\sigma_f = \text{const} = \sigma(T_f)$. Introduction of the conductivity jump is equivalent to introducing an effective ionization temperature T_i, which is essentially the profiling parameter. As usual in profiling, the value of T_0, which depends essentially on T_f, should be determined by substituting the profiling function into some equations belonging to the system or derivable from it.

We already know the solution at $\sigma = 0$ and const (see Sec. 1 of Ch. III): in a conductor at $x > 0$ we have $H, E \sim e^{-x/\delta}$, $S = S_0 \exp(-x/a)$, and $a = \delta/2$, where $S_0 = S_{-\infty}$ and δ are given by formulas (8) and (5). In front of the conductor at $x < 0$ we have $H = H_0$ and $S = S_0$. If the final plasma temperature T_f were known, then it would be possible to calculate from formula (8) the energy flux (power) and then from formula (27) the propagation velocity u.

For an approximate determination of the temperature T_f one can use an integral relation that is a generalization of the second integral possessed by the system in the static case (see Sec. 2 of Ch. III and formula (20)). This relation can be readily derived by multiplying (28) by $\sigma(T)$, replacing $\mathscr{T}$ and S by differential expressions (22) and (26), and integrating the resultant equation with respect to x from $-\infty$ to $+\infty$. We obtain

$$\int_0^{T_k} \sigma(T)\,\varkappa(T)\left[1 - \frac{\rho_0 u\,(w_f - w)}{\mathscr{T}}\right] dT = \left(\frac{In}{2}\right)^2. \tag{30}$$

In the static case $u = 0$ this equation goes over into (20). Relation (30), just like (20), is exact, but unlike the static case (in the case of a thin skin layer) it does not make it possible to determine the temperature T_f exactly, since the function $\mathscr{T}(T)$ is not known. However, it is possible to construct an approximate solution. Using the flux distribution $S = S_0 e^{-x/a}$ as the zeroth approximation, we obtain from (25) the temperature distribution $T(x)$ in the first approximation. Knowing $T(x)$, we obtain in the same approximation the function $\mathscr{T}(T) = -\kappa\,dT/dx$, and by substituting it in (20), we obtain an equation for T_f; this equation contains also T_0. A second equation for T_0 can be obtained by referring $T(x)$ to the point $x = 0$, namely $T_0 = T(0)$. As a result of these operations, we obtain the missing two equations for the unknown T_f and T_0. As already mentioned, S_0 and u are determined from Eqs. (8) and (27) (for more details see[39]).

It can be shown[39] that the formula for the rate of propagation of the discharge u reduces to a form characteristic of the heat-conduction mechanism of propagation, i.e., u is proportional to the temperature

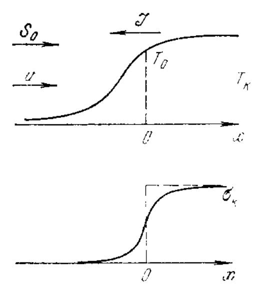

FIG. 15. Schematic distribution of T and σ; profiling of σ.

conductivity of the heated gas. The velocity u can also be represented in the form perfectly analogous with the Zel'dovich formula[15] for the flame propagation velocity.

Table II lists by way of illustration the results of calculations for air and argon at atmospheric pressure and a generator frequency $\nu = 15$ MHz.

The fact that the temperature interval $T_f - T_0$, in which the energy is relased, turns out to be quite narrow, is also evidence of an important analogy with the combustion process. As is well known, owing to the strong temperature dependence of the rate of the chemical reaction, the ignition temperature of the mixture differs only little from the final temperature of the products. The heat released in the reaction zone is transferred by heat conduction almost completely to the initial mixture and is consumed in heating this mixture to the ignition temperature.

The analogous situation in the discharge causes the balance equation (28) in the energy-release zone to differ little from the equation $\mathscr{T} + S = 0$, which corresponds to the static conditions, and the final temperature T_f is not much smaller than the maximal temperature T_m corresponding to the static regime with the same ampere turns (see Table II).

Thus, an analysis of a discharge in a stream has led to the essential conclusion that the plasma temperature depends little on whether the discharge occurs in immobile or in flowing gas. The temperature is determined only by the electric conductivity and thermal conductivity properties of the gas and by the ampere turns per unit length of the inductor.

3. The Real Process. Unsolved Problems

We have constructed above an idealized scheme, which has made it possible to explain certain regularities of the very complicated process of discharge in a gas stream. As seen from the foregoing, the theory is capable of providing an approximate answer to all the questions, if the geometry of the discharge and of the field is known. In fact, we can find the plasma temperature, the electromagnetic-energy flux density, and the gas-flux density in the discharge, and then, integrating over the surface of the front (formulas (29)), we can determine the power and the flow of the plasma. But this theory is unable to determine the geometry of the discharge. This is understandable, for the surface of the discharge front is established in accordance with the distribution of the axial velocities of the gas stream. Starting with the forward point of the "nose" of the discharge, at a given distribution of the

Table II

In, A-V/cm	H_0, Oe	T_m, 10^3 deg	T_f, 10^3 deg	T_0, 10^3 deg	w_f, kJ/g	σ_f, 10^{13} sec^{-1}	κ_f, 10^4 erg/cm·sec·deg	S_0, kw/cm^2	u, cm/sec	P, kW	G, cm^3/sec
Air											
19	24	7.2	7	6.4	26	0.24	40	0.085	2.6	8.5	260
37	46	8.9	8	7.1	38	0.66	35	0.20	4.1	20	410
53	66	10.4	9	6.9	43	1.38	12	0.27	4.9	27	490
60	76	11.0	10	7.6	48	2.18	10	0.28	4.6	28	450
72	91	11.9	11	8.8	53	2.92	13	0.36	5.2	36	520
94	119	13.0	12	10	62	3.71	18	0.54	6.9	54	680
Argon											
4.7	5.9	7.1	7	6.4	3.65	0.41	1.9	0.0040	0.62	0.4	62
10	13	8.1	8	7.3	4.23	1.35	2.5	0.011	1.5	1.1	150
20	25	9.1	9	8.1	4.96	2.34	3.6	0.031	3.5	3.1	350
32	40	10.3	10	8.8	6.06	3.15	5.2	0.070	6.5	7.0	650
52	65	11.6	11	9.5	8.17	3.87	7.0	0.16	11	16	1100
77	97	13.0	12	10.6	11.8	4.77	12	0.31	15	31	1500

external magnetic field, the surface aligns itself in such a way that the projection of the cold-gas velocity on the normal to the surface coincides exactly at the given radius, with the normal velocity of the discharge propagation. This condition determines the inclination of the surface to the axis at each point, i.e., the entire surface from the distribution of the axial velocity of the cold gas in the tube in the case of helical flow.

Unfortunately, this velocity distribution is still unknown, there being neither experimental data nor theory. A theoretical analysis poses certain difficulties, since it is necessary to take into account the viscosity of the gas and the deceleration by the wall of the tube, since the tube is long. Moreover, there is no theory that considers the complete picture of the gas flow with allowance for the heat release in the discharge zone. Such an investigation would also make it possible to understand better the mechanism of plasma recirculation, i.e., the drawing-in of the plasma far upstream, into the zone where there is certainly no magnetic field and there is consequently no current or energy release.

In order to estimate the value of the total power fed to the discharge, and the flow of gas that is transformed into plasma, on the basis of the idealized problem of normal flame propagation, let us assume that the discharge region is a cylinder of radius $R = 2$ cm and length $L = 8$ cm, independently of the power. The values of the power $P = 2\pi RLS_0$, and of the flow of gas transformed into a plasma, $G = u \cdot 2\pi RL$, are given in the last columns of Table II. These values are in qualitative agreement with the experimental data. We note that the plasma flow does not coincide with the gas flow, since part of the gas serves to press the discharge away from the tube walls and is not transformed into plasma.

The foregoing scheme does not take into account the radiation loss, i.e., it is applicable only to temperatures that are not too high, apparently not exceeding 10,000–12,000°. We cannot exclude the possibility that at very high temperatures the radiation, together with the ordinary thermal conductivity, takes part in the heating of the cold gas and in its preparation for "ignition," and this can affect the discharge propagation velocity.

4. Straight Flow

Let us return to the investigations[20,50], which were already referred to in the beginning of this chapter. In[12] no attention is paid at all to thermal conductivity or to any other mechanism of discharge propagation, and yet it is the propagation mechanism which determines the gas flow rate necessary to ensure a stationary "burning" of the discharge at the given operating conditions of the generator. At the same time, it is assumed arbitrarily that the plasma flow velocity at the emergence from the discharge zone is equal to the local velocity of sound. This condition has absolutely no basis whatever and in general disagrees with the experimental data, which indicate that the motion is subsonic, and the plasma outflow velocity does not exceed 100 m/sec.

Soshnikov, Trekhov, and Khoshev[50] considered a discharge with a straight and not helical gas flow, when the axial velocity of the cold gas in the tube was constant over the cross section (or maximal on the axis if the flow is of the Poiseuille type). The tube is inserted in a semi-infinite solenoid. The field inside the solenoid (at $z > 0$; the z axis coincides with the axis of the tube and of the solenoid) is described by Eqs. (2), as if the solenoid were infinite. The energy equation in this region is expressed in the form

$$\rho_0 u_0 c_p \frac{\partial T}{\partial z} = -\frac{1}{r}\frac{\partial}{\partial r} r\mathcal{J} + \sigma\langle E^2\rangle - \varphi, \quad \mathcal{J} = -\varkappa \frac{\partial T}{\partial r} \qquad (31)$$

(the notation is the same as before)*; here u_0 is the axial velocity of the cold gas. No account is taken in the equation of the heat flux in the axial direction. In order to justify this approximation, the authors assume that the rate of gas supply u_0 is large and the heating rate

$$\rho c_p \frac{dT}{dt} = \rho_0 u_0 c_p \frac{dT}{dz}$$

is much larger than the omitted term $-\frac{\partial}{\partial z}\kappa\frac{\partial T}{\partial z}$.

The region ahead of the solenoid, $z < 0$, is not considered at all, and instead a parabolic temperature profile with an arbitrarily chosen high temperature on

*Compare with Eqs. (13) and (22).

the axis, $T_0 = 5000-7000°K$, is specified at the entrance to the solenoid, at the section $z = 0$ (at sufficiently high T_0 the loss in the wall turns out to be larger than the heat release and the discharge does not develop). The velocity u_0 is also specified arbitrarily. The system of equations is solved numerically by approximately the same method as in the statistical case (see[34-36] and the beginning of Sec. 2 of Ch. III). The gas in the solenoid is heated, and the temperature reaches asymptotically a final value $T_m > T_0$ corresponding to the static regime with the same radius of the tube and the same ampere turns. By virtue of the similarity, which follows from Eq. (31) with the axial-thermal-conductivity term omitted, variation of the velocities u_0 brings about only a change in the characteristic length of the heating zone Δz. The results of the calculations are shown in Fig. 16.

The shortcomings of the described model become clear once the considerations advanced in Secs. 1–2 of Ch. IV are understood. In fact, it is thermal conductivity that serves as the mechanism of heating the cold gas to the "ionization" temperature, at which a sufficiently intense heat release can begin (in this case this is the temperature T_0 at the entry to the solenoid). More accurately, this role is played by axial heat flow in a direction opposite to the flow of the cold gas, and this is precisely what the authors have neglected. The gas-flow velocity u_0 is in this case not arbitrary but bounded from above.

The heat flux through the section $z = 0$ should heat the incoming cold gas to the ionization temperature, i.e., it is necessary to satisfy an energy-flux-equality condition of the type

$$\rho_0 u_0 w(T_0) = |J_z|_0 = \left(-\varkappa \frac{\partial T}{\partial z}\right)_{z=0} \qquad (32)$$

(strictly speaking, this equality must be integrated or averaged over the cross section). Owing to condition (32), the derivatives

$$\rho_0 u_0 c_p \frac{\partial T}{\partial z} \text{ and } \frac{\partial}{\partial z} \varkappa \frac{\partial T}{\partial z}$$

must also be comparable in the heating region, in contradiction to the proposition advanced in[50].

At large flow velocity, such that

$$\rho_0 u_0 c_p \frac{\partial T}{\partial z} \gg \frac{\partial}{\partial z} \varkappa \frac{\partial T}{\partial z},$$

it is simply impossible to attain the required temperature T_0 at the section $z = 0$, and no discharge is produced. In experiment, this situation gives the impression that the discharge ("flame") is "blown out" by the fast stream. Thus, for a more correct formulation of the problem it is necessary to take into account the axial heat conductivity and to include into consideration the zone ahead of the solenoid, or at least to specify at the section $z = 0$ not only the temperature T_0 but also the heat flux connected with u_0 by a condition of the type (32).

We must explain now the difference between straight and helical flows, by virtue of which we have disregarded the axial thermal conductivity when the latter was considered. In the case of helical flow, there is a vortical column in the central part of the tube; the axial velocity of the gas here is very small and part

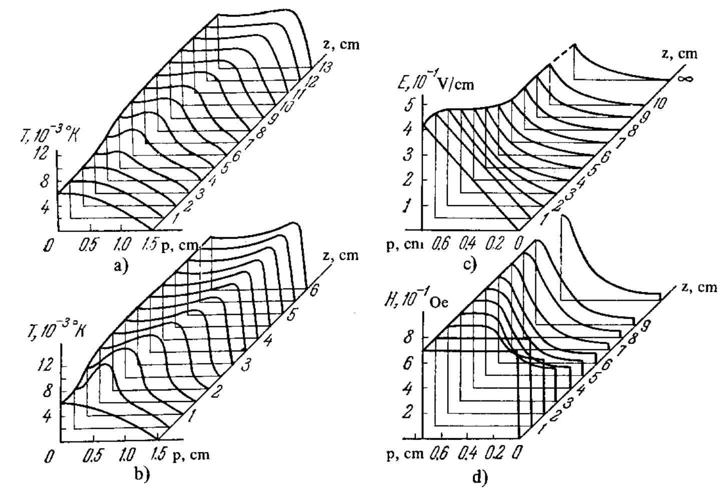

FIG. 16. Temperature and field distributions as calculated in [50]. Argon, flow 830 cm³/sec, the radius is denoted by ρ. a) In = 20 A-V/cm, $T_0 = 6000° K$, tube radius $\rho = 1.5$ cm; b) In = 55 A-V/cm, $T_0 = 6000° K$, $\rho_0 = 1.5$ cm; c) In = 55 A-V/cm, $T_0 = 7000° K$, $\rho_0 = 0.75$ cm; d) In = 55 A-V/cm, $T_0 = 7000° K$, $\rho_0 = 0.75$ cm.

of the gas may even flow upstream. Therefore the discharge is not "blown out" in the central part, and the axial heat flow does not play a significant role when the gas is heated to the "ionization" temperature. Almost the entire gas enters the discharge from the lateral surface, and the heating gives rise to the radial heat flux. In a straight-flow tube, on the other hand, the axial velocity in the central part is relatively large, and in spite of the appreciable role played by the radial heat flux and of the lateral inflow of the gas into the discharge, the tendency of the central part of the stream to "blow out" the discharge must of necessity counteract the heating action of the axial thermal conductivity.

In spite of the foregoing shortcomings, the calculations of[50] do give some idea of the temperature distribution in the heating region and agree qualitatively with experiment. To be sure, for comparison with the experimental data the authors had to decrease the velocity u_0 by one order of magnitude, to a value such that the quantities

$$\rho_0 u_0 c_p \frac{\partial T}{\partial z} \text{ and } \frac{\partial}{\partial z} \varkappa \frac{\partial T}{\partial z}$$

turned out to be comparable, since experiment, naturally, yielded precisely such a velocity u_0. However, the axial thermal conductivity apparently does not change radically the temperature distribution $T(z, r)$, since the calculated isotherms turned out to be similar to the experimental ones shown in Fig. 4.

The calculation results shown in Fig. 12 are quite useful also in that they demonstrate clearly how the discharge front is inclined relative to the flux (until the front practically reaches the walls of the tube). This circumstance was discussed in detail in Sec. 1 of Ch. IV. It is seen from Fig. 16 how the sharp rise (or maximum) of the temperature, i.e., the discharge layer, approaches the wall as the discharge is followed downstream. The projection of the stream velocity on the normal to the obtained oblique line of the discharge precisely corresponds to the normal velocity of propagation of the discharge referred to in Secs. 1–2 of Ch. IV.

The solution of the correctly formulated problem of straight flow would undoubtedly be of considerable interest for the understanding of the phenomena, although straight flow is hardly ever used in experiment, for too much heat goes off into the walls of the tube (this is also seen from Fig. 16).

[1]N. A. Kaptsov, Elektricheskie yavleniya v gazakh i vakuume (Electric Phenomena in Gases and Vacuum), Gsotekhizdat, 1950.

[2]J. J. Thomson, Phil. Mag. 2, 674 (1926); 4, 1128 (1927).

[3]G. I. Babat, Vestn. élektroprom. [Electric Industry Herald], No. 2, 1, No. 3, 2 (1942).

[4]G. I. Babat, J. Inst. Electr. Engrs. (Lond.) 94, 27 (1947).

[5]F. Cabannes, Ann. de phys. 10, 1026 (1955).

[6]G. Birkhoff, Zs. ang. Phys. 10, 204 (1958).

[7]H. J. Strauss, Ann. d. Phys. 1, 281 (1958).

[8]T. B. Reed, J. Appl. Phys. 32, 821 (1961).

[9]T. B. Reed, J. Appl. Phys. 34, 3146 (1963).

[10]T. B. Reed, J. Appl. Phys. 34, 2266 (1963).

[11]T. B. Reed, J. Appl. Phys. 32, 2534 (1961).

[12]A. Mironer and F. Hushfar, AIAA Electric Propulsion Conference in Colorado Springs, March 11–13, 1963.

[13]A. Mironer, Raktn. tekhn. i kosmonavtika (Rocket Engineering and Space Flight) 1, 225 (1963).

[14]S. V. Marinovskiĭ and A. J. Monroe, Investigations at High Temperatures, Trudy II. Mezhdunarodn. simpoziuma po vysokotemperaturnym issledovaniyam (Proc. of Second Internat. Symp. on High-temperature Research), Nauka, 1767, p. 73.

[15]B. M. Dymshitz and Ya. P. Koretskiĭ, Zh. Tekh. Fiz. 34, 1677 (1964) [Sov. Phys.-Tech. Phys. 9, 1294 (1965)].

[16]V. M. Gol'dfarb and S. V. Dresvin, Teplofiz. vysokikh temperatur (High-Temperature Physics) 3, 333 (1965).

[17]F. V. Vurzel', N. N. Dolgopolov, A. I. Maksimov, L. S. Polyak, and V. I. Fridman, Low Temperature Plasma, Proc. XX Internat. Congress on Theoretical and Applied Chemistry (Moscow, 1965), Russ. transl., Mir, 1967, p. 419.

[18]R. V. Mitin and K. K. Pryadkin, Zh. Teky, Fiz. 35, 1205 (1965) [Sov. Phys.-Tech. Phys. 10, 933 (1966).

[19]S. V. Dervskin, A. V. Donskoĭ, and V. M. Gol'dfarb, ibid. 35, 1646 (1965) [10, 1270 (1966)].

[20]R. E. Rovinskiĭ, L. E. Belousova, and V. A. Gruzdev, Teplofiz. vysokikh temperatur 4, 328 (1966).

[21]I. T. Alad'ev, I. G. Kulakov, O. L. Magdasiev, and L. P. Shatilov, Izv. SO AN SSSR, ser. tekhn. 10, (3), 50 (1966).

[22]F. Molinet, Compt. rend., Ser. B (1966).

[23]P. D. Jonston, Phys. Lett. 20, (51), 499 (1966).

[24]R. E. Rovinskiĭ, V. A. Gruzdev, T. M. Gutenmakher and A. P. Sobolev, Teplofiz, vysokikh temperatur 5, 557 (1967).

[25]D. W. Hughes,and E. R. Wooding, Phys. Lett. 24A, (1) 70 (1967).

[26]M. Ya. Smelyanskiĭ, S. V. Kononov, and M. I. Yakushin, Élektrotermiya No. 58, 15 (1967).

[27]M. Ya. Smelyanskiĭ, S. V. Kononov, and M. I. Yakushin, ibid. No. 61, 21 (1967).

[28]V. M. Gol'dfarb, A. V. Donskoĭ, S. V. Drevskin, and V. S. Klubnikin, Teplofiz. vysokikh temperatur 5, 549 (1967).

[29]M. Ya. Smelyanskiĭ, S. V. Kononov, and M. I. Yakushin, in: Elektrotermicheskie ustanovki (Electrothermal Apparatus), Izd. MEI, 1967.

[30]K. A. Egorova and A. I. Perevertun, Izv. SO AN SSSR ser. Khim. 3, (9) (1967).

[31]Yu. A. Buevich, V. M. Nikolaev, Yu. A. Plastinin, G. F. Sipachev, and M. I. Yakushin, Prikl. Mat. Teor. Fiz. No. 6, 111 (1968).

[32]S. I. Andreev, M. P. Vanyukov, A. A. Egorova, and B. M. Sokolov, Zh. Tekh. Fiz. 37, 1252 (1967) [Sov. Phys.-Tech. Phys. 12, 910 (1968)].

[33]M. P. Freeman and J. D. Chase, J. Appl. Phys. 39, (1), 180 (1968).

[34]V. N. Sochnikov and E. S. Trekhov, Teplofiz. vysokikh temperatur 4, 166 (1966).

[35]V. N. Sochnikov and E. S. Trekhov, ibid. 4, 324 (1966).

[36]V. N. Sochnikov and E. S. Trekhov, ibid. 5, 522 (1967).

[37]V. A. Gruzdev, R. E. Rovinskiĭ and A. P. Soboloev, Prikl. Mat. Teoret. Fiz. No. 1, 143 (1967).

[38]R. E. Rovinskiĭ and A. P. Soboloev, Teplofiz. vysokikh temperatur 6, 219 (1968).

[39]Yu. P. Raĭzer, Prikl. Mat. Teor. Fiz. No. 3, 3 (1968).

[40]S. V. Kononov and M. I. Yakushin, ibid. No. 6, 67 (1966).

[41]F. X. Powell, O. Fletcher, and E. R. Lippincoff, Rev. Sci. Instrum. 34 (1), 36 (1963).

[42]M. Plato, Zs. Naturforsch., XI, 9a (11), 1324 (1964).

[43]M. H. Clarkson, R. E. Field, and D. R. Keefer, AIAA Jorn. 4 (3), 546 (1966).

[44]A. V. Donskoi and S. V. Dresvin, Élektrotermiya No. 5, 37 (1963).

[45]Y. Reboux, Ingrs et techn. Nr. 166, 109 (1963).

[46]Y. Reboux, Ingrs. et techn., Nr. 157 (Sept. 1962); Rev. gen. d'electron., Nr. 196, 36 (1963).

[47]L. D. Landau and E. M. Lifshitz, Élektrodinamika sploshnykh sred (Electrodynamics of Continuous Media), Fizmatgiz, 1957 [Addison-Wesley, 1959].

[48]E. Jahnke, F. Emde, and F. Loesch, Special Functions (Russ. Transl.), Nauka, 1964.

[49]A. M. Vaĭnberg, Induktsionnye plavil'nye pechi (Induction Melting Furnaces), Energiya, 1967.

[50]V. N. Soshnikov, E. S. Trekhov, Yu. M. Khoshev in: Fizika gazorazryadnoĭ plazmy (Physics of Gas-discharge Plasma), No. 1, Atomizdat, 1968, p. 83.

[51]Ya. B. Zel'dovich, Teoriya goreniya i detonatsii gazov (Theory of Combustion and Detonation of Gases), AN SSSR, 1944.

[52]M. I. Yakushin, Prikl. Mat. Teor. Fiz. No. 3, 143 (1969).

[53]C. Sherman and J. F. McCoy, J. Appl. Phys. 36, 2080 (1965).

[54]A. J. Carswell, Rev. Sci. Instrum. 34, (9), 1015 (1963).

[55] P. J. Vermeulen, W. Lee Boddy, and F. A. Wierum, AJAA Journ. 5 (5), 1015, (1967).
[56] Yu. A. Buevich and M. I. Yakushin, Prikl. Mat. Teor. Fiz. No. 1, 56 (1968).
[57] Yu. A. Buevich, O. K. Egorov, and M. I. Yakushin, ibid. No. 4, 72 (1968).
[58] I. D. Cobine and D. A. Wilbur, J. Appl. Phys. 22, 835 (1951).
[59] V. P. Aksenov, L. M. Blinov, V. P. Marin, L. S. Polak, and V. S. Shchipachev. in: Kinetika i termodinamika khimicheskikh reaktsiĭ v nizkotemperaturnoĭ plazme (Kinetics and Thermodynamics of Chemical Reactions in Low-temperature Plasma) Nauka, 1965.
[60] P. A. Aresent'ev and E. F. Kustov, Teplofiz. vysokikh temperature 6, 44 (1968).

Translated by J. G. Adashko